
TSBOW: TRAFFIC SURVEILLANCE BENCHMARK FOR OCCLUDED VEHICLES UNDER VARIOUS WEATHER CONDITIONS

AAAI-26 MAIN TECHNICAL TRACK

✉ Ngoc Doan-Minh Huynh, Duong Nguyen-Ngoc Tran, Long Hoang Pham, Tai Huu-Phuong Tran,
Hyung-Joon Jeon, Huy-Hung Nguyen, Duong Khac Vu, Hyung-Min Jeon, Son Hong Phan,
Quoc Pham-Nam Ho, Chi Dai Tran, Trinh Le Ba Khanh, ✉ Jae Wook Jeon

Automation Lab, Department of Electrical and Computer Engineering
Sungkyunkwan University, Suwon, South Korea

{ngochdm, jwjeon}@skku.edu

January 22, 2026

ABSTRACT

Global warming has intensified the frequency and severity of extreme weather events, which degrade CCTV signal and video quality while disrupting traffic flow, thereby increasing traffic accident rates. Existing datasets, often limited to light haze, rain, and snow, fail to capture extreme weather conditions. To address this gap, this study introduces the **Traffic Surveillance Benchmark for Occluded vehicles under various Weather conditions (TSBOW)**, a comprehensive dataset designed to enhance occluded vehicle detection across diverse annual weather scenarios. Comprising over **32 hours** of real-world traffic data from densely populated urban areas, TSBOW includes more than **48,000 manually annotated** and **3.2 million semi-labeled frames**; bounding boxes spanning eight traffic participant classes from large vehicles to micromobility devices and pedestrians. We establish an object detection benchmark for TSBOW, highlighting challenges posed by occlusions and adverse weather. With its varied road types, scales, and viewpoints, TSBOW serves as a critical resource for advancing Intelligent Transportation Systems. Our findings underscore the potential of CCTV-based traffic monitoring, pave the way for new research and applications. The TSBOW dataset is publicly available at: <https://github.com/SKKUAutoLab/TSBOW>.

Keywords Computer Vision · Object Detection · Traffic Surveillance · Benchmark Dataset · Occluded Objects · Hostile Weathers

1 Introduction

Climate change has escalated the frequency and intensity of extreme weather events, significantly challenging computer vision tasks by degrading connection and image quality. These conditions disrupt traffic flow, increase traffic congestion and accident rates.

Analyzing traffic flow is essential for understanding traffic surveillance systems, enhancing transportation infrastructure through various applications. Public datasets and benchmarks have significantly advanced machine perception tasks, including image classification (Lu and Weng, Deng et al.), object detection (Zou et al., Lin et al.), object tracking (Yilmaz et al., Zhou et al.), semantic segmentation (Hafiz and Bhat, Gupta et al.).

Recent developments introduce specialized traffic datasets such as Dataset Quantization (Zhou et al.), compressed large datasets into smaller subsets; PointOdyssey (Zheng et al.), designed for long-term point tracking; TrafficCAM (Deng et al.), focused on traffic flow segmentation; and TUMTraf Video QA (Zhou et al.), targets unified spatio-temporal video understanding.



Figure 1: **Scenes from the TSBOW dataset**, comprising 198 videos recorded across four distinct scenarios spanning all seasons (sunny/cloudy, haze/fog, rain, snow) over a year. The dataset emphasizes adverse weather conditions and densely populated urban areas with heavy traffic, addressing significant challenges in image degradation and vehicle occlusion.

For object detection task, most existing traffic surveillance benchmarks rely on offline data captured using individual cameras, maintaining video quality in light rain or snow but proving inadequate under extreme weather conditions, such as heavy winds. Established object detection benchmarks, including UAVDT (Yu et al.) and UA-DETRAC (Wen et al.), cover sunny and light rainy conditions but exclude severe weather scenarios.

To advance traffic surveillance research, we introduce the **Traffic Surveillance Benchmark for Occluded vehicles under various Weather conditions (TSBOW)**, a comprehensive dataset derived from CCTV footage across diverse urban and highway routes. TSBOW encompasses a range of road types—urban streets, standard roads, and boulevards—with objects at fine, medium, and coarse scales, presenting significant challenges for detection models. Spanning a full year, the dataset captures a wide array of weather conditions, from clear skies to heavy snowfall, surpassing existing benchmarks in weather diversity (fig. 1).

Our primary contributions are outlined as follows:

- Development of a semi-automatic iterative annotation pipeline for efficient and accurate labeling (fig. 2).
- Introduction of TSBOW, a novel large-scale traffic surveillance dataset comprising 198 videos and over 3.2 million extracted frames across 145 regions of interest. Collected over four seasons, TSBOW includes diverse weather conditions, notably heavy haze and snow, and covers varied road types, including straight roads, intersections, shared lanes, overpasses, and constructions.
- Compilation of frames from densely populated areas with numerous, often occluded objects, posing significant challenges for object detection. The dataset includes diverse road types hosting eight object categories, including vehicles and pedestrians, with a balanced class distribution. Traffic lights and signs partially obscuring vehicles are also annotated, enhancing the differentiation of vehicle features from backgrounds.
- Manual annotation and verification of a substantial portion of the data by trained personnel for training, validation, and testing. Bounding boxes were independently labeled, cross-checked for consistency. The SOTA detection model is fine-tuned to annotate remaining frames.
- An object detection baseline for TSBOW provides a benchmark for real-time detection applications.

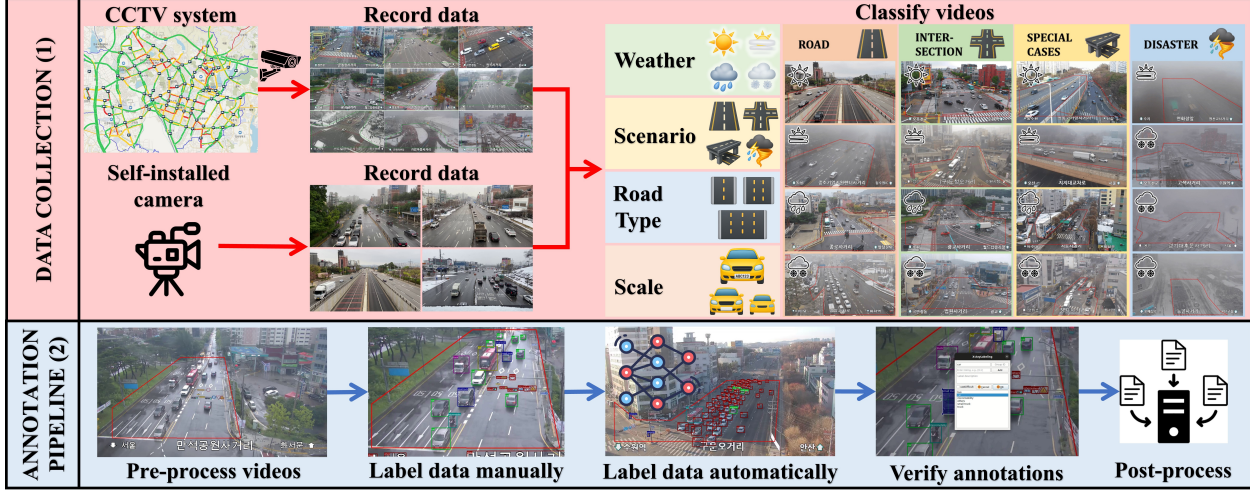


Figure 2: **Detailed overview of the data collection and annotation pipeline.** The process commences with the recording and categorization of videos during the data collection phase. Subsequently, the videos are preprocessed and allocated to a team of annotators for manual labeling. Next, a state-of-the-art model is fine-tuned to automatically annotate the remaining frames. The resulting annotations are then verified against predefined labeling criteria. Finally, the annotated instances are aggregated and undergo post-processing to finalize the dataset.

Dataset	Camera	Total Duration	Manually Labeled Fr.	Total Frames	Labeling Classes	Resolution	FPS			Unique Scenes			
							20	25	30	Sunny	Haze	Rain	Snow
UAVDT	UAVs	10 hrs	40,409	80K	3	1080 × 540	x			42	1	7	
UA-DETRAC	CCTV	10 hrs	—	140K	5	960 × 540		x		44		12	
AAURainSnow	CCTV	1.83 hrs	2,200	132K	-	640 × 480			x		1	5	16
TSBOW (ours)	CCTV	32.36 hrs	48,061	3.2M	8	1280 × 720	x	x	x	52	15	46	85

Table 1: Comparison of traffic surveillance datasets.

2 Related Works

2.1 Traffic Surveillance Dataset

Traffic surveillance systems depend on high-quality, diverse datasets to optimize performance Sun et al. [2024], Li et al. [2024], He et al. [2024]. Several public traffic datasets support this development, such as Waymo Sun et al. [2020], which provides 2D and 3D bounding boxes; TrafficMOT Liu et al. [2024], focused on multi-object tracking; eTram Verma et al. [2024], offering 2D bounding boxes for event-based cameras; STEP Weber et al. [2021], providing object segmentation and tracking; and OVT-B Liang and Han [2024], a benchmark for vocabulary multi-object tracking.

Recent advancements in autonomous driving frequently combine data from color cameras and LiDAR sensors. Color cameras capture visual details, such as color, texture, and semantic information, facilitating the creation of 2D bounding boxes. In contrast, LiDAR generates 3D spatial data, including distance, depth, and point clouds. Notable autonomous driving datasets include Ithaca365 Diaz-Ruiz et al. [2022] and SODA10M Han et al. [2021], which provide 3D bounding boxes; HoloVIC Ma et al. [2024], offering 3D bounding boxes and multi-object tracking; and TAP-Vid Doersch et al. [2022], which includes object tracking points in videos. Despite their complementary strengths, the integration of camera and LiDAR data presents notable limitations. First, LiDAR’s performance is limited by its height and coverage range, particularly when positioned at elevated locations, resulting in unreliable data. Second, LiDAR struggles to detect small objects, such as pedestrians and bicycles, at long distances due to sparse point clouds, which provide limited actionable information. Third, many existing traffic surveillance systems rely exclusively on color cameras, as incorporating LiDAR is often cost-prohibitive and impractical. Consequently, this research leverages existing government CCTV systems to analyze traffic flow across diverse weather conditions over a year, with a particular focus on disasters that significantly disrupt traffic.

The UAVDT dataset Yu et al. [2020] comprises 10 hours of UAV-captured video across urban areas under sunny and rainy conditions. This dataset presents detection challenges, including water puddle reflections, shadows, and camera motion blur, exacerbated by UAV altitudes ranging from low to high (above 70 meters), rendering it less applicable to ground-based surveillance like CCTV systems. Conversely, UA-DETRAC Wen et al. [2020] includes 10 hours of video recorded with a Canon camera Canon [2010] across 24 locations in China under four weather conditions (cloudy, nighttime, sunny, rainy). While sharing similar challenges—water puddles, shadows, and motion



Figure 3: Suwon recording locations in TSBOW dataset.

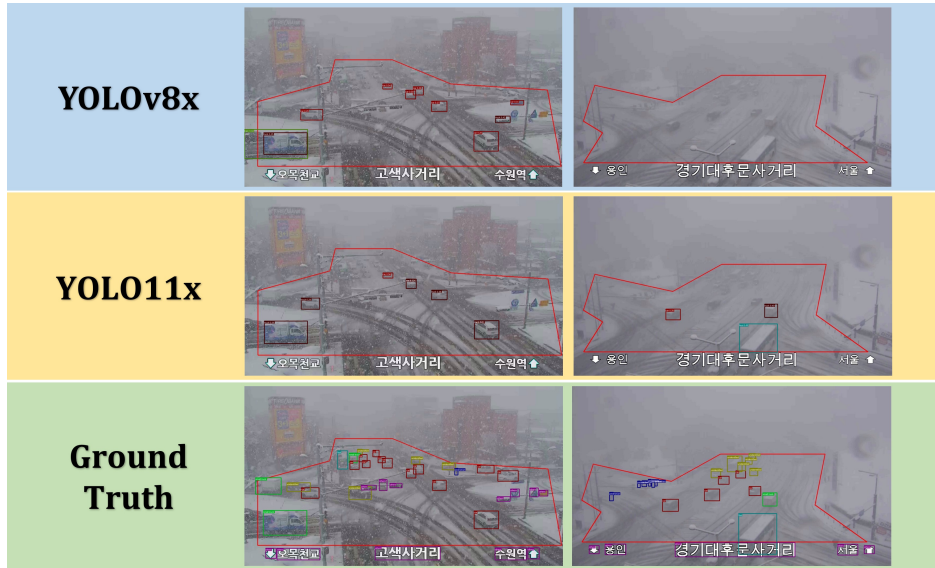


Figure 4: An example of detecting vehicles in heavy snow by using the YOLOv8x and YOLO11x models

blur—UA-DETRAC’s ground-proximate camera setup enhances model training performance but reduces complexity and real-world representativeness compared to UAVDT.

Both UAVDT and UA-DETRAC datasets are limited to sunny and rainy conditions, overlooking snowfall, a critical factor affecting video quality. Addressing this gap, the AAU RainSnow Traffic Surveillance Dataset Bahnson and Moeslund [2019] is introduced, captured using both a conventional RGB color camera and a thermal infrared camera. Comprising 22 five-minute videos, this dataset documents rainfall and snowfall across seven intersections in Denmark, providing segmentation for 13,297 objects under four weather conditions: rain, snow, haze, and fog, though it omits bounding boxes for vehicles. The AAU RainSnow dataset exhibits shared challenges with UAVDT and UA-DETRAC, including puddle reflections, raindrops on the lens, and camera variations. Like UA-DETRAC, its ground-proximate camera positioning reduces complexity, limiting its applicability to real-world traffic surveillance systems such as CCTV-based monitoring.

As shown in Tab. 1, compared to others, our dataset features longer video recordings and higher-quality traffic videos with higher-resolution frames. Additionally, it offers greater diversity in FPS, weather conditions, and scenarios compared to other benchmark datasets. Specifically, we include special scenarios and disaster cases that have not been covered in previous datasets. Because of limiting resources, we first focus on different weathers in day time, the night time will be updated in subsequent versions of our dataset.



Figure 5: An example of road types (RT) and scales (S)



Figure 6: Visualization of annotated instances of different classes in TSBOW dataset.

2.2 Object detection

Object detection Li et al. [2024] is a machine learning task that involves image localization and object classification. Several high-accuracy object detection models have been developed, such as Faster R-CNN Girshick [2015], Center-Net Duan et al. [2019], DETR (DEtection TRansformer) Carion et al. [2020]. However, when balancing processing speed and accuracy, the YOLO family of models emerges as a promising choice due to its exceptional performance and real-time processing capabilities. Various versions of YOLO have been proposed Hussain [2023], Hidayatullah et al. [2025] are introduced, such as YOLOv3 Zhao and Li [2020], YOLOv5 Olorunshola et al. [2023], YOLOv8 Sohan et al. [2024], YOLOX He et al. [2023], YOLOv11 Alkhammash [2025], and YOLOv12 Alif and Hussain [2025]. Compared to earlier versions, YOLOv8 features an enhanced backbone and employs a path aggregation network, achieving high accuracy while maintaining real-time processing. The YOLOv11 model further integrates vision transformers (ViTs) Khan et al. [2022] to enhance contextual understanding, yielding the highest accuracy in the mean Average Precision (mAP) metric, albeit with a slight reduction in processing speed. YOLOv12 combines FlashAttention and an R-ELAN backbone to achieve higher accuracy without compromising real-time detection. RT-DETR Zhao et al. [2024], leveraging a transformer architecture, excels in dense and complex scene understanding. In this study, we employ YOLOv8, YOLOv11, YOLOv12, and RT-DETR, specifically the x-large variants, to establish experimental baselines for the Traffic Surveillance Benchmark for Occluded vehicles under various Weather conditions (TSBOW).

3 CCTV Traffic Surveillance Benchmark

The Traffic Surveillance Benchmark for Occluded vehicles under various Weather conditions (TSBOW) dataset is specifically engineered to capture traffic flow within the diverse road networks of Suwon city, Gyeonggi, Korea.

3.1 Collection Routes

Our dataset is derived from fixed routes comprising a wide range of scenes (fig. 3), enabling robustness evaluation under diverse weather conditions. It is systematically classified according to distinct attributes, including scenario, weather, road type, and scale. Detailed descriptions are provided below.

First, the video scenarios are categorized into four distinct types—road, intersection, special case, and disaster—as illustrated in fig. 1.

- **Road** comprises straight roads or those where traffic flow remains unaffected by traffic lights.
- **Intersection** includes three subtypes—T, Y, or crossroad—and extends to scenes where traffic lights or pedestrian crossings influence traffic flow, thereby warranting classification as intersections.
- **Special case** includes videos featuring shared lanes, overpasses, or mid-road construction. Shared lanes, including narrow one-way variants, are characterized by bidirectional traffic and pedestrian activity within a

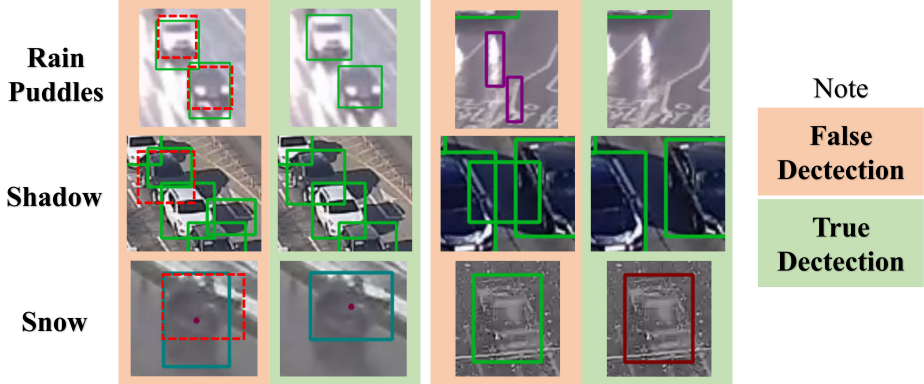


Figure 7: Challenges by Weather Conditions in TSBOW.

Scenario/Weather	Normal	Haze	Rain	Snow	Total
Road	12	6	15	28	61
Intersection	28	6	25	37	96
Special cases	12	2	6	11	31
Disaster	—	1	—	9	10
Total	52	15	46	85	198

Table 2: Statistics on scenarios and weathers in TSBOW.

single lane, prevalent in space-constrained, densely populated areas. Overpass footage is subdivided into two groups: scenes solely depicting the overpass and those capturing both the overpass and adjacent or underlying roads. The latter poses greater detection challenges due to significant scale disparities among vehicles within a single frame.

- **Disaster** pertains to scenarios where hostile weather severely degrades video quality, such as heavy snow, rendering vehicle identification exceedingly difficult and presenting the most formidable challenge for detection models. Fig. 4 illustrates the object detection outcomes using YOLOv8x and YOLOv11x.

Second, videos for the TSBOW dataset, covering roads, intersections, and special cases, were recorded in Suwon under diverse weather conditions—normal (sunny), haze, rain, and snow—throughout the year. Unlike prior datasets where “rain” videos resemble sunny conditions due to wet roads without visible raindrops, TSBOW classifies “rain” only when raindrops or active rainfall are evident. Similarly, “snow” videos require visible snowflakes or snowfall, altering object appearances (e.g., vehicles with white pixels from snow or frost). These conditions, combined with unstable connections and camera vibrations from strong winds, degrade video quality and complicate computer vision tasks. Videos with wet roads or residual snow lacking active precipitation are classified as “normal” (sunny). In the disaster scenario, heavy haze and extreme snow significantly impair object detection by obscuring visual features, as shown in fig. 4. Snow-covered vehicles blend into white snowy backgrounds, challenging model performance and object-background differentiation. Termed “disaster” due to its severe impact on traffic flow, this scenario exacerbates congestion and accident rates.

Third, the TSBOW dataset classifies data collection zones by the number of straight lanes per direction, excluding turning lanes, into three road types: urban (two lanes, primarily cars, small trucks, and pedestrians), standard (four lanes, including larger vehicles like trailer trucks), and boulevard (over six lanes, featuring flatbed trucks and car transporters). Unlike other datasets limited to urban and standard roads, TSBOW includes boulevards, where high vehicle density and occlusion intensify detection challenges due to frequent object overlap.

Final, CCTV cameras along routes and intersections vary in angle and height, producing bounding box sizes categorized into three scales: fine (near road surface, detailed object visualization), medium (elevated cameras, discernible license plates but reduced clarity), and coarse (distant cameras, high vehicle count but partial visibility due to distance and occlusion). Fig. 5 provides an example of road types and scales. While UA-DETRAC covers fine and medium scales, UAVDT focuses on medium and coarse scales.

The diverse attributes of our dataset—spanning locations (fig. 3), weather conditions, road types, and object scales (fig. 5)—render it a robust resource for assessing and enhancing traffic surveillance systems. Furthermore, it incorporates eight labeling classes, surpassing other benchmark datasets in granularity, facilitating detailed classification of vehicles and pedestrians and fostering deeper insights into traffic dynamics for infrastructure improvement. Beyond object detection, the TSBOW dataset supports additional applications, including crowd counting Li et al. [2021], speed

Road Type/Scale	Fine	Medium	Coarse	Total
Urban	14	66	9	89
Standard	13	61	4	78
Boulevard	2	20	9	31
Total	29	147	22	198

Table 3: Statistics on scales and road types in the TSBOW.

Instances	UAVDT Ground Truth	UA-DETRAC Ground Truth	TSBOW Ground Truth	Manually Labeled
Car	756,166	1,052,408	50,269,953	783,203
Bus	0	95,570	2,252,616	35,715
Truck	0	20,641	565,932	10,657
Small Truck	-	105,436	3,258,031	58,272
Pedestrian	-	-	2,935,102	53,414
Micromobility	-	-	1,691,744	29,959
Unidentified	-	-	515,447	8,379
Others	0	-	9,648,223	151,556
Total	756,166	1,274,055	71,137,048	1,131,155

Table 4: Instance statistics across UAVDT, UA-DETRAC, and TSBOW datasets.

estimation Fernández Llorca et al. [2021], and object tracking Soleimanitaleb et al. [2019], thereby offering practical utility for real-world traffic management systems.

3.2 Labeling Process

The annotation process for the TSBOW dataset ensures high-quality ground truth data through five phases: video pre-processing, manual labeling, automatic labeling, annotation verification, and post-processing. Firstly, in pre-processing, regions of interest (ROIs) are defined to capture the main road sections where traffic objects are most visible. After that, frames are then extracted at set intervals and manually annotated using X-Anylabeling Wang [2023], an open-source tool for precise bounding box creation, focusing on vehicles and pedestrians in high-density urban roads and intersections. Subsequently, a YOLOv12x model trained on region-specific vehicle characteristics (e.g., size, shape, color) in Korea, is used for semi-automatic labeling of remaining frames. Annotations undergo rigorous review and quality control to eliminate substandard entries, ensuring high-quality data. Lastly, the annotated images are compiled and subjected to post-processing to produce the final version of the dataset.

Objects within the TSBOW dataset are classified into eight distinct categories: *car*, *bus*, *truck*, *small truck*, *micromobility*, *pedestrian*, *unidentified*, and *others*. Annotated examples across these categories are depicted in fig. 6.

In the first version of the dataset, which is aimed for public release, 48,061 frames have been manually labeled and verified. The annotations for remaining frame from over 3.2M were generated using the YOLOv12x model. Subsequent versions will substantially increase the proportion of manually annotated frames. License plates and pedestrian faces have been obscured to comply with privacy regulations.

3.3 Dataset Statistic and Characteristics

This study analyzes data statistics under two conditions: contextual influences and road structures. Tab. 2 details video counts by scenario and weather, with intersections—impacted by traffic lights and pedestrians—exhibiting more occluded objects, prompting increased data collection. Video distribution across scenes remains balanced, comparable to other scenarios. Tab. 3 categorizes videos by scale and road type, with urban and standard roads prevailing over boulevards due to the city-zone focus. CCTV cameras, primarily offering medium-scale perspectives, are strategically placed to capture traffic dynamics, with sufficient fine- and coarse-scale videos to cover diverse scenarios.

As previously noted, our dataset comprises over 3.2 million frames across 198 videos. Tab. 4 details the bounding box counts for each class in three datasets: UAVDT, UA-DETRAC, and our TSBOW. Of the 1.1 million manually annotated objects, cars constitute 69%, with camera information and traffic signs contributing to the proportion of other objects. Unlike benchmark datasets, where cars exceed 83%, our dataset achieves a more balanced distribution across eight classes. The high prevalence of pedestrians and micromobility devices indicates recordings from densely populated urban areas. Frames average 24 objects, with a maximum of 122. The highest number of semi-labeled bounding boxes in a single video reaches 1,233,828 across 17,789 frames, reflecting frequent object occurrences. Bounding boxes are classified by occlusion level, measured as the percentage of area occluded: no occlusion (<15% IoU), light occlusion (15-<40% IoU), and heavy occlusion ($\geq 40\%$ IoU). Their distribution is 721,684 (no occlusion),

Subset	Total	Training	Validation	Test
Manually labeled frames	48,061	10,881	7,559	29,621
Total frames	3,267,598	973,877	658,856	1,634,865

Table 5: Statistics of manually labeled and total video frames across training, validation, and test subsets.

Method	Precision	Recall	mAP50	mAP50-95
YOLOv8x	0.783	0.705	0.733	0.609
YOLO11x	0.786	0.696	0.734	0.614
YOLOv12x	0.806	0.662	0.744	0.615
RT-DETR-x	0.731	0.740	0.718	0.552

Table 6: Model performances after training 100 epochs and validating with $\text{imgsz}=1280$ on manually labeled test set.

266,420 (light occlusion), and 143,051 (heavy occlusion). Accordingly, traffic flow is categorized into light (44 videos), moderate (98 videos), and heavy (56 videos). This substantial instance count and balanced class distribution enhance the dataset’s reliability for traffic surveillance research.

In our TSBOW dataset, numerous factors challenge detection models in accurately identifying and localizing objects, as outlined below:

- Weather conditions: Normal weather scenarios—cloudy and sunny—impact detection performance. Cloudy conditions eliminate vehicle shadows on road surfaces, simplifying detection. In contrast, sunny conditions introduce shadows, leading to less precise bounding boxes that encompass both vehicles and their shadows, reducing model accuracy (fig. 7). Haze degrades image quality, obscuring object features and further complicating detection. Rainy conditions create water puddles that distort bounding box sizes, while strong winds and unstable connections during rain or snow induce camera movement, causing motion blur.
- Scenarios: Continuous traffic flow on roads and overpasses enhances detection model performance due to minimal vehicle occlusions. However, simultaneous recording of overpasses and underlying or adjacent roads complicates detection due to varying vehicle scales and viewing angles. Conversely, traffic lights disrupt flow, causing significant occlusions where only partial objects are visible, posing substantial challenges for models in localizing vehicles and often failing to detect highly occluded instances. Road construction further exacerbates occlusions by reducing lanes, leading to traffic congestion. These issues, compounded by disaster scenarios, underscore the detection difficulties discussed.

These characteristics collectively impede the precision and reliability of object detection models across diverse environmental and situational contexts. **More detailed descriptions are mentioned in the Supplementary material.**

4 Experiments

4.1 Object Detection Qualitative Result

In this section, we establish benchmarks for the TSBOW dataset using neural network-based object detection methods. We utilize YOLOv8x, YOLO11x, YOLOv12x, and RT-DETR-x models, pretrained on the COCO dataset Lin et al. [2014] and fine-tuned on our dataset at an image resolution of 1280 pixels, as lower resolutions impair inference performance, particularly for occluded vehicles. Evaluation metrics include average precision (AP), mean average precision (mAP), intersection over union (IoU), precision, and recall.

Each video is segmented into three subsets: the first 5 minutes for testing, the next 2 minutes for validation, and the final 3 minutes for training, with frame details provided in Tab. 5. To ensure reliable model performance, manually labeled sets are used for training, validation, and testing. Inference parameters include an IoU threshold of 0.6, an image size of 1280 pixels, and a confidence score of 0.5.

Tab. 6 illustrates the precision, recall, mAP50, and mAP50-95 scores of the YOLOv8x, YOLO11x, YOLOv12x, and RT-DETR-x models after training for 100 epochs. In the evaluation, RT-DETR-x achieves the highest recall, prioritizing broad object coverage, but exhibits lower precision and mAP scores, indicating weaker localization performance. Conversely, YOLOv12x outperforms others in precision, mAP50, and mAP50-95, attributed to its reduced false positive rate. Thus, YOLOv12x demonstrates superior robustness for general object detection, and was selected to annotate the remaining frames.



Figure 8: Selected scenes for comparison with other datasets

Method	Precision	Recall	mAP50	mAP50-95
YOLOv12x trained on UAVDT	0.647	0.141	0.383	0.328
YOLOv12x trained on UA-DETRAC	0.820	0.295	0.558	0.459
YOLOv12x trained on TSBOW (ours)	0.743	0.869	0.846	0.792

Table 7: Models performance for *car* across different metrics **on the comparison set**.

4.2 Datasets Comparison

To ensure a fair comparison, we created a subset of medium-scale scenes distinct from the TSBOW dataset, featuring unique road structures and vehicle characteristics. While snowy conditions were recorded in Suwon, additional videos capturing normal, haze, and rain conditions were collected in Seoul (Fig. 8). Unlike UA-DETRAC, which includes only fine- and medium-scale videos captured by a color camera, and UAVDT, which focuses on medium- and coarse-scale drone footage, TSBOW encompasses fine, medium, and coarse scales. Therefore, the comparison subset comprises medium-scale scenes, included in the UAVDT, UA-DETRAC, and TSBOW datasets.

Tab. 7 details detection performance for the *car* class across various metrics on this comparison set. YOLOv12x models were trained on UAVDT, UA-DETRAC, and TSBOW datasets with identical setups. The UAVDT-trained model yielded the lowest scores, as its high-altitude drone footage is less applicable to ground-based CCTV surveillance. The UA-DETRAC-trained model achieved high precision but low recall, mAP50, and mAP50-95, due to its emphasis on clear vehicle features at specific distances, overlooking distant vehicles. Conversely, TSBOW mitigates these limitations by incorporating vehicles across diverse scales and optimizing region-of-interest (ROI) settings to enhance detection. Consequently, the TSBOW-trained model balances precision and recall, achieving superior performance in recall, mAP50, and mAP50-95.

4.3 Ablation Study on Object Classes

Tab. 8 presents the detailed detection performance of the fine-tuned YOLOv12x model across various object classes. The class “car,” with high occurrence, achieves the highest scores in three of four metrics, while “bus” excels in mAP50-95 due to the distinct features of fixed-shape objects. For smaller objects, such as “pedestrians” and “micromobility,” the model demonstrates promising detection performance.

4.4 Ablation Study on Data Characteristics

The fine-tuned YOLOv12x model is evaluated across diverse data characteristics, including weather, scenario, scale, road type, and traffic. Tab. 9 provides detailed performance metrics, including precision, recall, mAP50, and mAP50-95. In the “disaster” scenario, heavy snow significantly obscures object features, markedly impairing detection. Under weather conditions, “normal” yield lower scores than “rain” due to frequent vehicle overlap. Similarly, the “coarse” scale, characterized by numerous small and heavily occluded objects, poses significant detection challenges. For road

Class	Images	Instances	Precision	Recall	mAP50	mAP50-95
All	29,621	689,839	0.806	0.662	0.744	0.615
Unidentified	2,177	4,855	0.475	0.223	0.317	0.221
Others	14,248	90,276	0.769	0.628	0.696	0.619
Pedestrian	11,807	32,779	0.833	0.605	0.715	0.447
Micromobility	9,124	18,490	0.793	0.574	0.726	0.519
Car	29,244	479,560	0.959	0.932	0.959	0.849
Bus	12,378	21,037	0.917	0.929	0.951	0.876
Small truck	16,176	36,152	0.878	0.830	0.870	0.750
Truck	5,390	6,690	0.824	0.575	0.720	0.643

Table 8: YOLOv12x performance across different classes.

Group	Category	Precision	Recall	mAP50	mAP50-95
Scenario	Road	0.756	0.608	0.687	0.575
	Intersection	0.827	0.677	0.759	0.633
	Special cases	0.800	0.681	0.747	0.615
	Disaster	0.765	0.559	0.656	0.510
Weather	Normal	0.791	0.622	0.726	0.605
	Haze	0.799	0.732	0.785	0.684
	Rain	0.851	0.721	0.789	0.664
	Snow	0.783	0.641	0.723	0.597
Scale	Fine	0.733	0.619	0.686	0.559
	Medium	0.810	0.666	0.751	0.630
	Coarse	0.791	0.676	0.733	0.581
Road Type	Urban	0.821	0.675	0.757	0.632
	Standard	0.828	0.661	0.754	0.622
	Boulevard	0.745	0.664	0.702	0.579
Traffic	Light	0.792	0.658	0.726	0.617
	Moderate	0.795	0.647	0.734	0.606
	Heavy	0.841	0.678	0.769	0.640

Table 9: Influence of dataset characteristics on object detection performance

type, “boulevards,” with high vehicle density and occlusion, present substantial obstacles to detection accuracy. Object detectors often struggle with heavily occluded objects, frequently misidentifying two to three occluded vehicles as a single object, leading to numerous missed detections.

5 Conclusion and Future Works

This study introduces the Traffic Surveillance Benchmark for Occluded vehicles under various Weather conditions (TSBOW), a comprehensive, semi-automatically annotated traffic surveillance dataset designed to improve monitoring system training, particularly under extreme weather conditions such as heavy haze and snow. Collected across all seasons and diverse road scenarios, TSBOW comprises 32 hours of footage from 198 videos, encompassing a variety of road types and scales, and providing multiple viewing angles for vehicles and pedestrians. The dataset includes over 3.2 million frames, each annotated with weather conditions and scenarios, alongside detailed object annotations derived from extracted images. Capturing complex, high-density scenes of vehicles and pedestrians in crowded urban settings, TSBOW features approximately 71.1 million bounding boxes across eight distinct traffic participant classes. As a robust resource for traffic surveillance research, TSBOW offers substantial potential to deepen insights into traffic dynamics and support advancements in intelligent transportation systems. The initial version focuses on daytime traffic flow under varying weather conditions. Future versions will include ground truth annotations for nighttime scenarios and additional computer vision tasks, such as multi-object tracking, semantic segmentation, vehicle counting, and speed estimation, to further enhance its utility.

Acknowledgments

This work was supported by the Institute of Information & communications Technology Planning & Evaluation (IITP) grant funded by the Korea government (MSIT) (No. 2021-0-01364, An intelligent system for 24/7 real-time traffic surveillance on edge devices).

References

Dengsheng Lu and Qihao Weng. A survey of image classification methods and techniques for improving classification performance. *International journal of Remote sensing*, 28(5):823–870, 2007.

Jia Deng, Wei Dong, Richard Socher, Li-Jia Li, Kai Li, and Li Fei-Fei. Imagenet: A large-scale hierarchical image database. In *2009 IEEE Conference on Computer Vision and Pattern Recognition*, pages 248–255, 2009. doi:10.1109/CVPR.2009.5206848.

Zhengxia Zou, Keyan Chen, Zhenwei Shi, Yuhong Guo, and Jieping Ye. Object detection in 20 years: A survey. *Proceedings of the IEEE*, 111(3):257–276, 2023.

Tsung-Yi Lin, Michael Maire, Serge Belongie, James Hays, Pietro Perona, Deva Ramanan, Piotr Dollár, and C. Lawrence Zitnick. Microsoft coco: Common objects in context. In David Fleet, Tomas Pajdla, Bernt Schiele, and Tinne Tuytelaars, editors, *Computer Vision – ECCV 2014*, pages 740–755, Cham, 2014. Springer International Publishing. ISBN 978-3-319-10602-1.

Alper Yilmaz, Omar Javed, and Mubarak Shah. Object tracking: A survey. *Acm computing surveys (CSUR)*, 38(4):13–es, 2006.

Bolei Zhou, Hang Zhao, Xavier Puig, Sanja Fidler, Adela Barriuso, and Antonio Torralba. Scene parsing through ade20k dataset. In *Proceedings of the IEEE Conference on Computer Vision and Pattern Recognition (CVPR)*, July 2017.

Abdul Mueed Hafiz and Ghulam Mohiuddin Bhat. A survey on instance segmentation: state of the art. *International journal of multimedia information retrieval*, 9(3):171–189, 2020.

Agrim Gupta, Piotr Dollár, and Ross Girshick. Lvis: A dataset for large vocabulary instance segmentation. In *2019 IEEE/CVF Conference on Computer Vision and Pattern Recognition (CVPR)*, pages 5351–5359, 2019. doi:10.1109/CVPR.2019.00550.

Daquan Zhou, Kai Wang, Jianyang Gu, Xiangyu Peng, Dongze Lian, Yifan Zhang, Yang You, and Jiashi Feng. Dataset quantization. In *Proceedings of the IEEE/CVF International Conference on Computer Vision*, pages 17205–17216, 2023.

Yang Zheng, Adam W Harley, Bokui Shen, Gordon Wetzstein, and Leonidas J Guibas. Pointodyssey: A large-scale synthetic dataset for long-term point tracking. In *Proceedings of the IEEE/CVF International Conference on Computer Vision*, pages 19855–19865, 2023.

Zhongying Deng, Yanqi Cheng, Lihao Liu, Shujun Wang, Rihuan Ke, Carola-Bibiane Schönlieb, and Angelica I Aviles-Rivero. Trafficciam: A versatile dataset for traffic flow segmentation. *IEEE Transactions on Intelligent Transportation Systems*, 2024.

Xingcheng Zhou, Konstantinos Larintzakis, Hao Guo, Walter Zimmer, Mingyu Liu, Hu Cao, Jiajie Zhang, Venkatarayanan Lakshminarasimhan, Leah Strand, and Alois Knoll. TUMTraf videoQA: Dataset and benchmark for unified spatio-temporal video understanding in traffic scenes. In *Forty-second International Conference on Machine Learning*, 2025. URL <https://openreview.net/forum?id=Yfoi5O68rf>.

Hongyang Yu, Guorong Li, Weigang Zhang, Qingming Huang, Dawei Du, Qi Tian, and Nicu Sebe. The unmanned aerial vehicle benchmark: Object detection, tracking and baseline. *International Journal of Computer Vision*, 128:1141–1159, 2020.

Longyin Wen, Dawei Du, Zhaowei Cai, Zhen Lei, Ming-Ching Chang, Honggang Qi, Jongwoo Lim, Ming-Hsuan Yang, and Siwei Lyu. Ua-detrac: A new benchmark and protocol for multi-object detection and tracking. *Computer Vision and Image Understanding*, 193:102907, 2020. ISSN 1077-3142. doi:<https://doi.org/10.1016/j.cviu.2020.102907>. URL <https://www.sciencedirect.com/science/article/pii/S1077314220300035>.

Zhihong Sun, Guoheng Wei, Wei Fu, Mang Ye, Kui Jiang, Chao Liang, Tingting Zhu, Tao He, and Mithun Mukherjee. Multiple pedestrian tracking under occlusion: A survey and outlook. *IEEE Transactions on Circuits and Systems for Video Technology*, 2024.

Yiming Li, Yi Wang, Wenqian Wang, Dan Lin, Bingbing Li, and Kim-Hui Yap. Open world object detection: a survey. *IEEE Transactions on Circuits and Systems for Video Technology*, 2024.

Jinpeng He, Huaixin Chen, Biyuan Liu, Sijie Luo, and Jie Liu. Enhancing yolo for occluded vehicle detection with grouped orthogonal attention and dense object repulsion. *Scientific Reports*, 14(1):19650, 2024.

Pei Sun, Henrik Kretzschmar, Xerxes Dotiwalla, Aurelien Chouard, Vijaysai Patnaik, Paul Tsui, James Guo, Yin Zhou, Yuning Chai, Benjamin Caine, et al. Scalability in perception for autonomous driving: Waymo open dataset. In *Proceedings of the IEEE/CVF conference on computer vision and pattern recognition*, pages 2446–2454, 2020.

Lihao Liu, Yanqi Cheng, Zhongying Deng, Shujun Wang, Dongdong Chen, Xiaowei Hu, Pietro Liò, Carola-Bibiane Schönlieb, and Angelica Aviles-Rivero. Trafficmot: A challenging dataset for multi-object tracking in complex traffic scenarios. In *Proceedings of the 32nd ACM International Conference on Multimedia*, MM '24, page 1265–1273. Association for Computing Machinery, 2024. ISBN 9798400706868. doi:10.1145/3664647.3681153. URL <https://doi.org/10.1145/3664647.3681153>.

Aayush Atul Verma, Bharatesh Chakravarthi, Arpitsinh Vaghela, Hua Wei, and Yezhou Yang. Etram: Event-based traffic monitoring dataset. In *Proceedings - 2024 IEEE/CVF Conference on Computer Vision and Pattern Recognition, CVPR 2024*, Proceedings of the IEEE Computer Society Conference on Computer Vision and Pattern Recognition, pages 22637–22646. IEEE Computer Society, 2024. doi:10.1109/CVPR52733.2024.02136.

Mark Weber, Jun Xie, Maxwell D. Collins, Yukun Zhu, Paul Voigtlaender, Hartwig Adam, Bradley Green, Andreas Geiger, Bastian Leibe, Daniel Cremers, Aljosa Osep, Laura Leal-Taixé, and Liang-Chieh Chen. STEP: segmenting and tracking every pixel. *CoRR*, abs/2102.11859, 2021. URL <https://arxiv.org/abs/2102.11859>.

Haiji Liang and Ruize Han. Ovt-b: A new large-scale benchmark for open-vocabulary multi-object tracking. In A. Globerson, L. Mackey, D. Belgrave, A. Fan, U. Paquet, J. Tomczak, and C. Zhang, editors, *Advances in Neural Information Processing Systems*, volume 37, pages 14849–14863. Curran Associates, Inc., 2024. URL https://proceedings.neurips.cc/paper_files/paper/2024/file/1addeeac24ce6168e20bcee85645720e9-Paper-Datasets_and_Benchmarks_Track.pdf.

Carlos A. Diaz-Ruiz, Youya Xia, Yurong You, Jose Nino, Junan Chen, Josephine Monica, Xiangyu Chen, Katie Luo, Yan Wang, Marc Emond, Wei-Lun Chao, Bharath Hariharan, Kilian Q. Weinberger, and Mark Campbell. Ithaca365: Dataset and driving perception under repeated and challenging weather conditions. In *Proceedings of the IEEE/CVF Conference on Computer Vision and Pattern Recognition (CVPR)*, pages 21383–21392, June 2022.

Jianhua Han, Xiwen Liang, Hang Xu, Kai Chen, Lanqing HONG, Chaoqiang Ye, Wei Zhang, Zhenguo Li, Xiaodan Liang, and Chunjing Xu. SODA10m: Towards large-scale object detection benchmark for autonomous driving, 2021. URL <https://openreview.net/forum?id=kUkp7WdUny9>.

Cong Ma, Lei Qiao, Chengkai Zhu, Kai Liu, Zelong Kong, Qing Li, Xueqi Zhou, Yuheng Kan, and Wei Wu. Holovic: Large-scale dataset and benchmark for multi-sensor holographic intersection and vehicle-infrastructure cooperative. In *Proceedings of the IEEE/CVF Conference on Computer Vision and Pattern Recognition (CVPR)*, pages 22129–22138, June 2024.

Carl Doersch, Ankush Gupta, Larisa Markeeva, Adria Recasens, Lucas Smaira, Yusuf Aytar, Joao Carreira, Andrew Zisserman, and Yi Yang. Tap-vid: A benchmark for tracking any point in a video. In S. Koyejo, S. Mohamed, A. Agarwal, D. Belgrave, K. Cho, and A. Oh, editors, *Advances in Neural Information Processing Systems*, volume 35, pages 13610–13626. Curran Associates, Inc., 2022. URL https://proceedings.neurips.cc/paper_files/paper/2022/file/58168e8a92994655d6da3939e7cc0918-Paper-Datasets_and_Benchmarks.pdf.

Canon. Canon eos 500d. https://www.canon.co.uk/for_home/product_finder/cameras/digital_slr/eos_550d/, 2010. Accessed: December 25, 2024.

Chris Holmberg Bahnsen and Thomas B. Moeslund. Rain removal in traffic surveillance: Does it matter? *I E E E Transactions on Intelligent Transportation Systems*, 20(8):2802–2819, August 2019. ISSN 1524-9050. doi:10.1109/TITS.2018.2872502.

Ross Girshick. Fast r-cnn. In *Proceedings of the IEEE international conference on computer vision*, pages 1440–1448, 2015.

Kaiwen Duan, Song Bai, Lingxi Xie, Honggang Qi, Qingming Huang, and Qi Tian. Centernet: Keypoint triplets for object detection. In *Proceedings of the IEEE/CVF international conference on computer vision*, pages 6569–6578, 2019.

Nicolas Carion, Francisco Massa, Gabriel Synnaeve, Nicolas Usunier, Alexander Kirillov, and Sergey Zagoruyko. End-to-end object detection with transformers. In *European conference on computer vision*, pages 213–229. Springer, 2020.

Muhammad Hussain. Yolo-v1 to yolo-v8, the rise of yolo and its complementary nature toward digital manufacturing and industrial defect detection. *Machines*, 11(7), 2023. ISSN 2075-1702. doi:10.3390/machines11070677. URL <https://www.mdpi.com/2075-1702/11/7/677>.

Priyanto Hidayatullah, Nurjannah Syakrani, Muhammad Rizqi Sholahuddin, Trisna Gelar, and Refdinal Tubagus. Yolov8 to yolo11: A comprehensive architecture in-depth comparative review. *arXiv preprint arXiv:2501.13400*, 2025.

Liquan Zhao and Shuaiyang Li. Object detection algorithm based on improved yolov3. *Electronics*, 9(3):537, 2020.

Oluwaseyi Ezekiel Olorunshola, Martins Ekata Irhebhude, and Abraham Eseoghene Evwiekpae. A comparative study of yolov5 and yolov7 object detection algorithms. *Journal of Computing and Social Informatics*, 2(1):1–12, 2023.

Mupparaju Sohan, Thotakura Sai Ram, Rami Reddy, and Ch Venkata. A review on yolov8 and its advancements. In *International Conference on Data Intelligence and Cognitive Informatics*, pages 529–545. Springer, 2024.

Qiyi He, Ao Xu, Zhiwei Ye, Wen Zhou, and Ting Cai. Object detection based on lightweight yolox for autonomous driving. *Sensors*, 23(17):7596, 2023.

Eman H Alkhammash. Multi-classification using yolov11 and hybrid yolo11n-mobilenet models: A fire classes case study. *Fire*, 8(1):17, 2025.

Mujadded Al Rabbani Alif and Muhammad Hussain. Yolov12: A breakdown of the key architectural features, 2025. URL <https://arxiv.org/abs/2502.14740>.

Salman Khan, Muzammal Naseer, Munawar Hayat, Syed Waqas Zamir, Fahad Shahbaz Khan, and Mubarak Shah. Transformers in vision: A survey. *ACM computing surveys (CSUR)*, 54(10s):1–41, 2022.

Yian Zhao, Wenyu Lv, Shangliang Xu, Jinman Wei, Guanzhong Wang, Qingqing Dang, Yi Liu, and Jie Chen. Detrs beat yolos on real-time object detection. In *Proceedings of the IEEE/CVF Conference on Computer Vision and Pattern Recognition (CVPR)*, pages 16965–16974, June 2024.

Bo Li, Hongbo Huang, Ang Zhang, Peiwen Liu, and Cheng Liu. Approaches on crowd counting and density estimation: a review. *Pattern Analysis and Applications*, 24:853–874, 2021.

David Fernández Llorca, Antonio Hernández Martínez, and Iván García Daza. Vision-based vehicle speed estimation: A survey. *IET Intelligent Transport Systems*, 15(8):987–1005, 2021.

Zahra Soleimanitaleb, Mohammad Ali Keyvanrad, and Ali Jafari. Object tracking methods: A review. In *2019 9th International Conference on Computer and Knowledge Engineering (ICCKE)*, pages 282–288. IEEE, 2019.

Wei Wang. Advanced auto labeling solution with added features. <https://github.com/CVHub520/X-AnyLabeling>, 2023.

Pavan Yadav. Tips for labeling images for object detection models. <https://www.esri.com/arcgis-blog/products/arcgis-pro/geoai/tips-for-labeling-images-for-object-detection-models/>, 2023. Accessed: December 01, 2024.

Waymo LLC. Waymo open dataset labeling specifications. https://github.com/waymo-research/waymo-open-dataset/blob/master/docs/labeling_specifications.md, 2023. Accessed: November 20, 2024.

Yihao Xie and Felipe Rodríguez. Zero-emission integration in heavy-duty vehicle regulations: A global review and lessons for china. *The international council on clean transportation*, 2021.

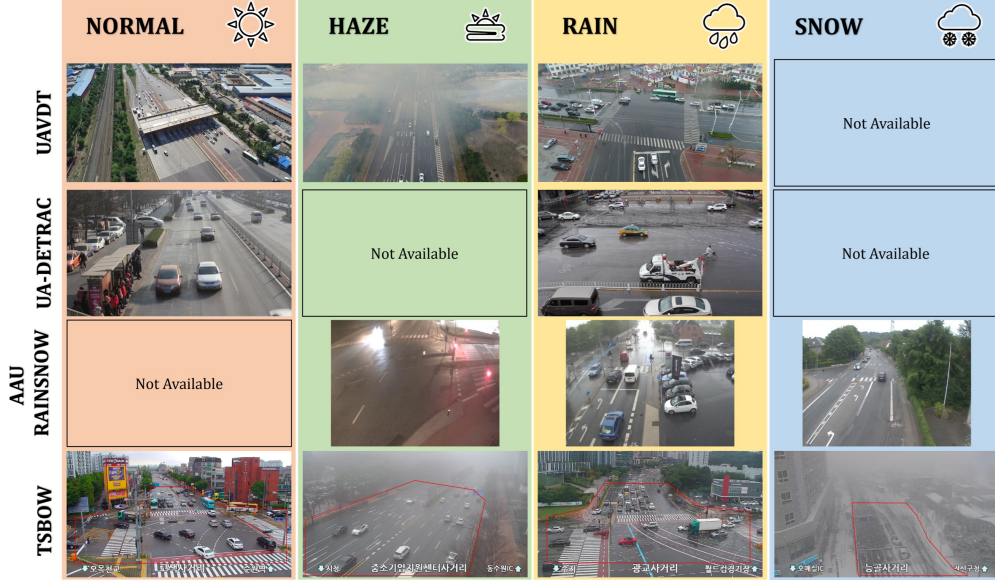


Figure 1: Comparison with other datasets about weather conditions and scales

Supplementary Materials

1 Related Works

Fig. 1 compares weather conditions and scales across the TSBOW dataset and other datasets, including UAVDT, UA-DETTRAC, and AAURainSnow. UA-DETTRAC and AAURainSnow consists solely of fine- and medium-scale videos captured using a color camera, whereas UAVDT, utilizing drone footage, concentrates exclusively on medium and coarse scales. In contrast, the TSBOW dataset encompasses all three scales—fine, medium, and coarse—offering greater diversity.

2 The TSBOW Dataset

2.1 Labeling Criteria

Labeling criteria Yadav [2023], LLC [2023], are as follows:

- Bounding boxes must tightly encase objects to accurately capture their shapes and locations, minimizing extraneous background inclusion.
- Occluded objects are labeled as fully visible to enable recognition despite partial obscurement.
- A vehicle is deemed within the Region of Interest (ROI) if its bounding box center resides therein.
- Traffic signs and lights overlapping vehicles are classified as "others" to differentiate background elements from vehicle features.
- Objects transported by trucks are separately annotated to ensure detection of conveyed vehicles.
- Objects moved by pedestrians are labeled as "others," reflecting their road space occupancy while distinguishing them from standard vehicle categories and aiding differentiation from background elements.

2.2 Data Format and Description

The TSBOW dataset comprises videos in MP4 format and extracted frames in JPEG format to minimize re-encoding loss, accompanied by corresponding YOLO label text files for each image. Each label file entry adheres to the bounding box format, specifying the class ID, X and Y coordinates (center point), width, and height. Data for training, validation, and test sets are supplied in text format, supplemented by a YAML file detailing dataset metadata.



Figure 2: Comparison weather conditions and disaster



Figure 3: Car accident in the TSBOW dataset

2.3 Train-Test Split

Videos capture intervals between red-light phases, each lasts approximately two minutes. The three-minute training splits include vehicle flows and queues. The extended five-minute testing splits capture more flows for comprehensive evaluation. Also, varied CCTVs provide diverse viewpoints, mitigating over-optimistic results from similarities.

2.4 Differentiation of Weather Conditions and “Disaster” Scenarios

Fig. 2 distinguishes between “haze” and “snow” in other weather condition and “haze” and “snow” in “disaster” conditions. The fog and snowflakes in “haze” and “snow” have minimal impact on object features and traffic flow. In “disaster” conditions, heavy haze and heavy snow obscures object features, reduces detection accuracy, disrupts traffic, and increases accident frequency.

Additionally, a recorded car accident in snowy conditions highlights the impact of slippery roads (as shown in fig. 3).

2.5 Detailed Description of Object Classes

- *car* category includes sedan, SUV, and van, while *bus* includes both small bus and standard bus.
- *small truck*, comparable in size to SUV or van, comprises pickup truck, small truck, and small box truck.
- *micromobility* denotes bicycle, motorbike, and scooter, and *pedestrian* annotations are restricted to individuals on crosswalk.

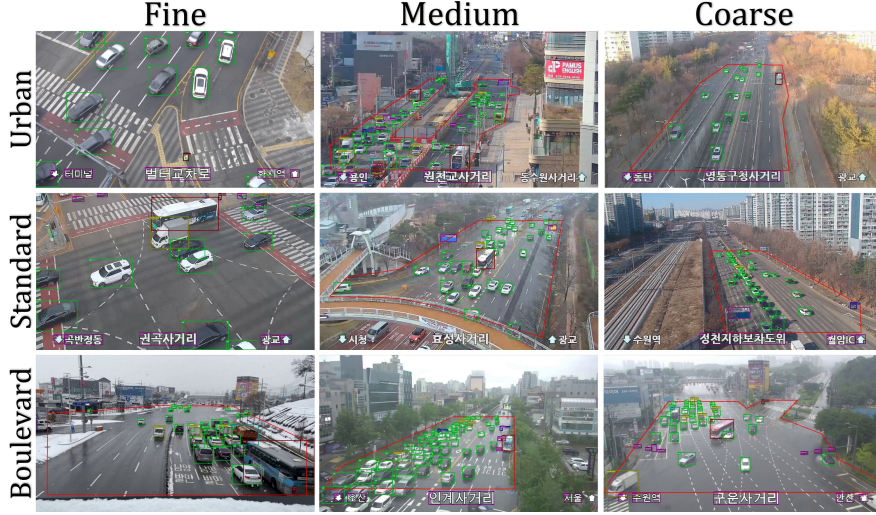


Figure 4: Examples of Road Types and Scales in the TSBOW dataset



Figure 5: Intersections under different viewpoints in diverse weather conditions

- *truck* is the most diverse vehicle category Xie and Rodríguez [2021], including large box truck, trailer truck, flatbed truck, dump truck, tanker truck, concrete truck, garbage truck, crane truck, tow truck, fire truck, and car transporter.
- In hostile weather conditions, unstable network connections may result in indistinct or corrupted vehicle visuals, which are designated as *unidentified*.
- Traffic signs and lights partially obscuring vehicles are separately annotated as *others* to distinguish vehicle features from background elements.
- Vehicles clearly visible yet not fitting predefined categories are also labeled as *others*.

2.6 Diverse Road Types and Scales

Fig. 4 illustrates examples of various road types and scales within the TSBOW dataset.

2.7 Varied Field of View (FOV)

Fig. 5 depicts identical intersections captured from different viewpoints and under diverse weather conditions. These videos encompass all three scales—fine, medium, and coarse—enhancing its representational diversity.

Subset	no_occlusion	light_occlusion	heavy_occlusion
Train	166,437	62,090	33,996
Val	114,680	43,727	22,057
Test	440,567	160,603	86,998
Total	721,684	266,420	143,051

Table 1: Distribution of instances by occlusion level across training, validation, and test sets.

Method	Image Size	Precision	Recall	mAP50	mAP50-95
YOLOv8x	960	0.796	0.683	0.730	0.606
	1120	0.804	0.694	0.739	0.616
	1280	0.783	0.705	0.733	0.609
	1440	0.800	0.704	0.744	0.620
	1600	0.798	0.705	0.745	0.618
YOLO11x	960	0.789	0.677	0.729	0.608
	1120	0.798	0.686	0.739	0.618
	1280	0.786	0.696	0.734	0.614
	1440	0.797	0.694	0.742	0.620
	1600	0.797	0.698	0.743	0.620
YOLOv12x	960	0.825	0.629	0.732	0.601
	1120	0.815	0.650	0.740	0.612
	1280	0.806	0.662	0.744	0.615
	1440	0.802	0.665	0.744	0.615
	1600	0.797	0.668	0.743	0.613
RT-DETR-x	960	0.722	0.703	0.697	0.437
	1120	0.738	0.725	0.718	0.516
	1280	0.731	0.740	0.718	0.552
	1440	0.742	0.742	0.725	0.532
	1600	0.734	0.733	0.716	0.493

Table 2: Validation of model performance with different image sizes on a manually labeled test set.

2.8 Occlusion Distribution

Tab. 1 details the occlusion distribution of instances across training, validation, and test sets.

3 Experiments

3.1 Experiment Environment

Experiments were conducted on a system operating Ubuntu 22.04, equipped with an Intel Core i9-10980XE CPU (3.00GHz), 256GB of RAM, and four NVIDIA RTX A6000 GPUs (each with 48GB of memory).

3.2 Model Training and Inference Details

- For model training, the hyperparameters were: $imgsz = 1280$, $epochs = 100$, SGD optimizer, $lr = 0.01$, $patience = 50$, $momentum = 0.937$. For validation, the parameters were: $conf = 0.5$, $IoU = 0.6$, $max_detect = 300$, $batch = 32$. Validation was conducted across multiple image sizes: 960, 1120, 1280, 1440, and 1680. Tab. 2 provides detailed model performance after validating with different image sizes.
- For inference on the remaining frames, $conf = 0.6$ was applied to small objects (pedestrian and micromobility), while $conf = 0.3$ was used for other classes. The higher confidence score for pedestrians addresses challenges associated with significant overlap when crossing streets, whereas the lower score for other classes enhances the detection of small objects, particularly those near the boundaries of the region of interest (ROI).

3.3 Model Performances under Different Weather Conditions

Fig. 6 presents the performance of models on a manually labeled test set under various weather conditions, following training for 100 epochs on the training set.

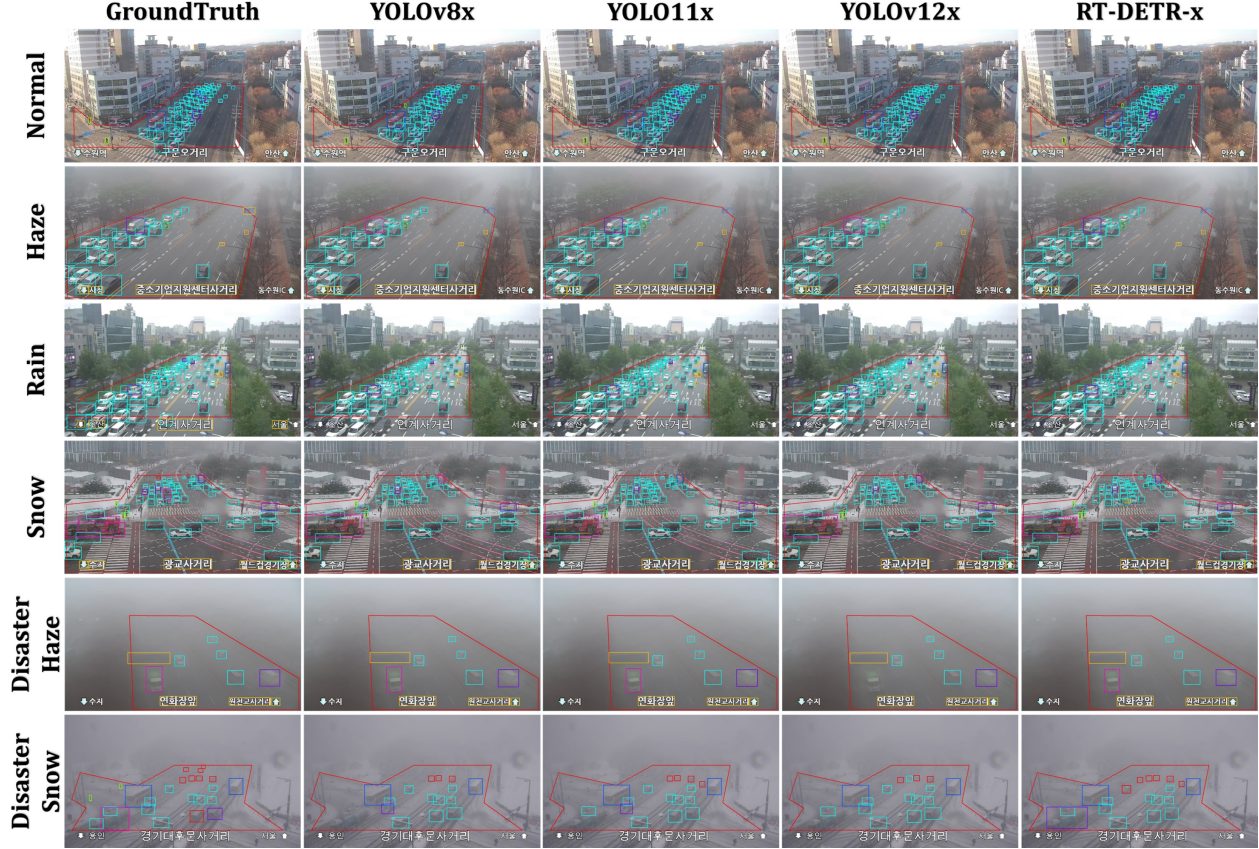


Figure 6: Model performances under different weather conditions

Weather	Scenario	Scale	RoadType	Location
normal	special case	medium	urban	Seoul
haze	intersection	medium	urban	Seoul
rain	intersection	medium	standard	Seoul
snow	road	medium	standard	Suwon

Table 3: Environmental and road scenario metadata for selected conditions.

3.4 Impact of “Disaster” Scenarios on Model Performance

In extreme weather conditions, vehicles often appear as indistinct shadows, leading object detection models to misclassify them as part of the background.

- Small vehicles at a distance during heavy snowfall frequently appear as gray polygons devoid of distinct features. Consequently, models often fail to classify these as objects, even when an “unidentified” class is available. Additionally, white vehicles are frequently undetected in snowy conditions due to their color blending with the snow-covered background. The pre-trained models exhibit poor performance in such conditions, whereas fig. 6 illustrates improved detection accuracy after fine-tuning. Pre-trained models commonly overlook “unidentified” objects, leading users to erroneously perceive the road as empty or sparsely traffic, despite potentially high vehicle volumes on the route. This misdetection has significant implications, as it impedes the government’s ability to promptly manage traffic in response to accidents or congestion caused by degraded road surface conditions.
- In conditions of extreme haze, image quality is severely compromised by heavy noise, obscuring vehicle features. As a result, models typically detect only those vehicles in close proximity to the camera. Vehicles at greater distances are often missed, as only their lights remain visible, while other parts blend into the hazy background.

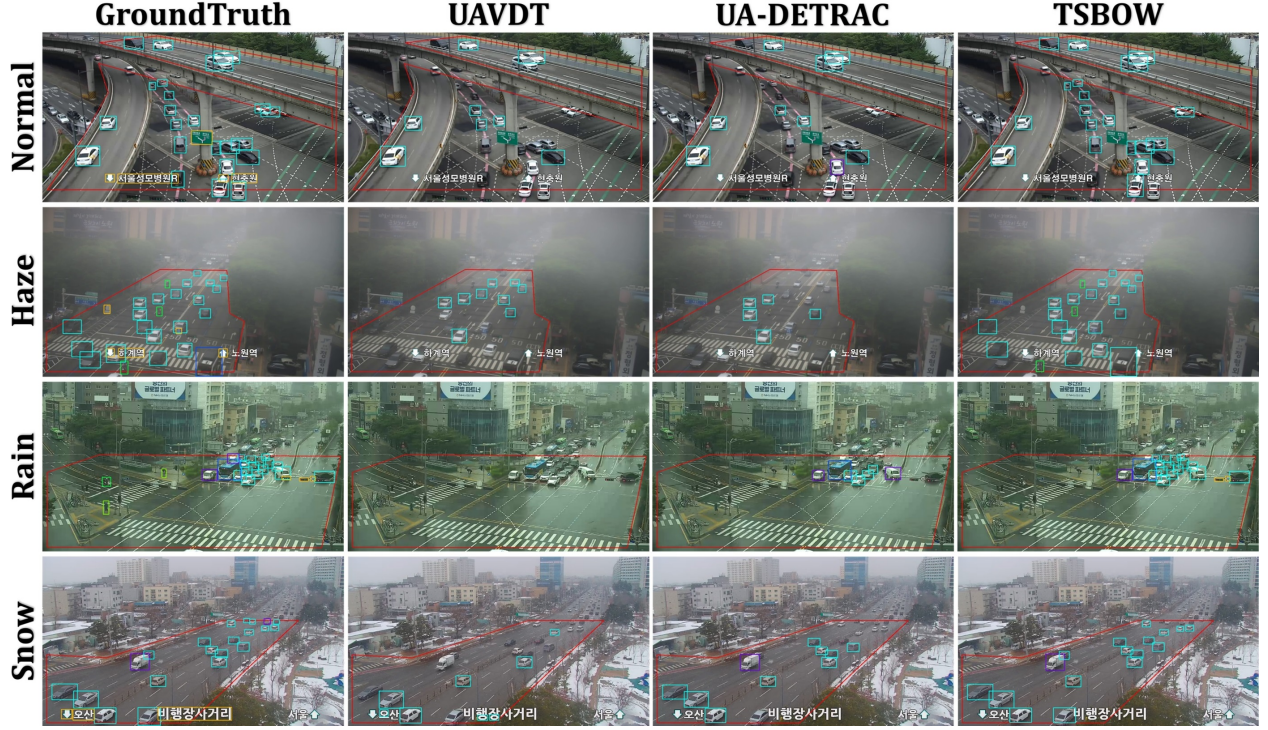


Figure 7: Model performances when training on different datasets

3.5 Model Performance Across Datasets

Tab. 3 details the comparison set, encompassing weather conditions, scenarios, scales, road types, and locations. As the "medium" scale is common across all datasets, it is selected for the comparison set.

Fig. 7 illustrates a comparative analysis of model performance when trained on different datasets.